

Improved QCD Form Factor Constraints and $\Lambda_b \rightarrow \Lambda_c \ell \bar{\nu}$

C. Glenn Boyd* and Richard F. Lebed[†]

Department of Physics
University Of California, San Diego
La Jolla, California 92093-0319

We construct model-independent parametrizations of the individual QCD form factors relevant to $\Lambda_b \rightarrow \Lambda_c \ell \bar{\nu}$ decays. These results follow from dispersion relations and analyticity, and incorporate an improvement in the technique that reduces the number of necessary parameters. To describe most form factors with 5%–10% accuracy over the entire kinematic range, three parameters are necessary, one of which is its normalization at zero recoil. We also apply the improvement to meson decays, and find, using the heavy quark form factor normalization, that almost every $\bar{B} \rightarrow D \ell \bar{\nu}$ and $\bar{B} \rightarrow D^* \ell \bar{\nu}$ form factor is well-described by a single-variable parametrization. $\bar{B} \rightarrow \pi \ell \nu$ requires a total of only 3 to 5 parameters, depending on the desired accuracy.

Final Version: October, 1996

* gboyd@ucsd.edu

[†] rlebed@ucsd.edu

1. Introduction

Considerable theoretical and experimental attention has been devoted to the extraction of the Cabibbo–Kobayashi–Maskawa element $|V_{cb}|$ from both exclusive and inclusive semileptonic decays of the B meson. Because of the key role this parameter plays in the investigation of rare decays and CP violation in the third quark generation, it is important to make as many independent determinations of $|V_{cb}|$ as possible. The baryonic semileptonic decay $\Lambda_b \rightarrow \Lambda_c \ell \bar{\nu}$ provides an opportunity to extract $|V_{cb}|$ in a fashion as theoretically clean as in $\bar{B} \rightarrow D \ell \bar{\nu}$ or $\bar{B} \rightarrow D^* \ell \bar{\nu}$, because heavy quark symmetry[1–3] predicts for both cases a single universal form factor in the heavy quark limit[4], including the normalization of $1 + \mathcal{O}(1/m_c^2)$ at zero recoil[5,6].

The prospect for experimentally determining the q^2 dependence of $\Lambda_b \rightarrow \Lambda_c \ell \bar{\nu}$ form factors is promising, because the method applied by ALEPH[7] to $\bar{B} \rightarrow D^* \ell \bar{\nu}$ should work equally well[8] for baryons. The cumulative data sets of ALEPH, DELPHI, and OPAL[9] contain about 250 Λ_b semileptonic events; an additional 200 events have been observed at CDF[10]. This raises the possibility of extracting $|V_{cb}|$ from baryon decays.

To fully exploit this possibility, a model-independent parametrization of the $\Lambda_b \rightarrow \Lambda_c \ell \bar{\nu}$ form factors is desirable. This is important because the kinematic rate vanishes at zero recoil, so an extrapolation of the data based on some parametrization is required.

In this paper we apply the parametrization imposed by QCD on the physical form factors. The requirement of compatibility with QCD is obtained through the application of dispersion relations based on the analyticity properties of form factors as functions of the momentum transfer variable. The method of extracting information on amplitudes by this form of complex analysis is quite old[11], and has been applied to the study of semileptonic decays of light mesons in a more contemporary language in Ref. [12]. Its application to heavy quark systems has received much attention in more recent years[13–19].

In general, these applications say little about the overall normalization of form factors, but encode a great deal of information about the shape. The expression of this information manifests itself in a simple parametrization[17,18] that spans the functional space of form factors allowed by QCD dispersion relations. In this work we apply the parametrization, supplemented by a new development presented here, to the decay $\Lambda_b \rightarrow \Lambda_c \ell \bar{\nu}$.

The technical development introduced for $\Lambda_b \rightarrow \Lambda_c \ell \bar{\nu}$ also has important implications for form factors in meson decays such as $\bar{B} \rightarrow D^{(*)} \ell \bar{\nu}$ and $\bar{B} \rightarrow \pi \ell \bar{\nu}$. It allows one to obtain form factor parametrizations with smaller uncertainties and fewer parameters than those discussed in earlier works[17,18].

The paper is organized as follows: In Sec. 2 we outline the derivation of form factor bounds from QCD dispersion relations and introduce the technical improvement that strengthens our constraints. We construct the form factor parametrization that obeys these bounds, and discuss the inclusion of heavy resonances, in Sec. 3. In Sec. 4 we discuss the numerics of the heavy resonance masses and obtain information on the quality of parametrizations for $\Lambda_b \rightarrow \Lambda_c \ell \bar{\nu}$ form factors. Section 5 describes the implications of our technical improvement to meson decays. We conclude in Sec. 6.

2. Dispersion Relation Inequalities

The QCD matrix elements governing the semileptonic decay $\Lambda_b \rightarrow \Lambda_c \ell \bar{\nu}$ may be expressed in terms of form factors defined by

$$\begin{aligned}\langle \Lambda_c(p') | V^\mu | \Lambda_b(p) \rangle &= \bar{u}_c(p') [F_1 \gamma^\mu + F_2 v^\mu + F_3 v'^\mu] u_b(p), \\ \langle \Lambda_c(p') | A^\mu | \Lambda_b(p) \rangle &= \bar{u}_c(p') [G_1 \gamma^\mu + G_2 v^\mu + G_3 v'^\mu] \gamma_5 u_b(p),\end{aligned}\tag{2.1}$$

where $v = p/M_{\Lambda_b}$ and $v' = p'/M_{\Lambda_c}$ are meson velocities, $V^\mu = \bar{c}\gamma^\mu b$ and $A^\mu = \bar{c}\gamma^\mu \gamma_5 b$ are polar and axial vector flavor-changing currents, and the form factors are functions of the momentum transfer $q^2 = (p - p')^2$. In terms of these form factors, the differential decay width for $\Lambda_b \rightarrow \Lambda_c \ell \bar{\nu}$ with a massless charged lepton ℓ is

$$\frac{d\Gamma}{dq^2} = \frac{|V_{cb}|^2 G_F^2 (k^2 q^2)^{\frac{1}{2}}}{96\pi^3 M^3} \left\{ (Q_-) [2q^2 |F_1|^2 + M^2 |H_V|^2] + (Q_+) [2q^2 |G_1|^2 + M^2 |H_A|^2] \right\},\tag{2.2}$$

where the terms proportional to $|F_1|^2$ and $|G_1|^2$ alone give the partial widths for transversely polarized intermediate W bosons[20], whereas

$$\begin{aligned}H_V(q^2) &= \frac{1}{M} \left[(M + m) F_1 + \frac{Q_+}{2} \left(\frac{F_2}{M} + \frac{F_3}{m} \right) \right], \\ H_A(q^2) &= \frac{1}{M} \left[(M - m) G_1 - \frac{Q_-}{2} \left(\frac{G_2}{M} + \frac{G_3}{m} \right) \right],\end{aligned}\tag{2.3}$$

are the partial wave amplitudes for a longitudinally polarized W 's, with

$$Q_\pm = (M \pm m)^2 - q^2.\tag{2.4}$$

The factor

$$k^2 = \frac{M^2}{q^2} \mathbf{p}_c^2 = \frac{1}{4q^2} Q_+ Q_- \tag{2.5}$$

is an invariant kinematic quantity related to the three-momentum \mathbf{p}_c of the Λ_c in the rest frame of the decaying Λ_b , and $M, m = M_{\Lambda_b}, M_{\Lambda_c}$, respectively. The form factor combinations $(\frac{F_2}{M} - \frac{F_3}{m})$ and $(\frac{G_2}{M} - \frac{G_3}{m})$, which appear with the Lorentz structure q^μ , give contributions to the rate proportional to the lepton mass squared m_ℓ^2 , and are consequently mainly of interest for constraining models.

We begin our derivation of constraints from dispersion relations following the well-known methods developed by the authors listed in Refs. [11,12]. In QCD, the two-point function of a flavor-changing current $J = V, A$, or $V - A$,

$$\Pi_J^{\mu\nu}(q) = (q^\mu q^\nu - q^2 g^{\mu\nu})\Pi_J^T(q^2) + g^{\mu\nu}\Pi_J^L(q^2) \equiv i \int d^4x e^{iqx} \langle 0 | T J^\mu(x) J^{\dagger\nu}(0) | 0 \rangle, \quad (2.6)$$

can be rendered finite by making one subtraction, leading to the dispersion relations

$$\chi_J^{T,L}(q^2) \equiv \frac{\partial \Pi_J^{T,L}}{\partial q^2} = \frac{1}{\pi} \int_0^\infty dt \frac{\text{Im} \Pi_J^{T,L}(t)}{(t - q^2)^2}. \quad (2.7)$$

The functions $\chi_J^{T,L}(q^2)$ may be computed reliably in perturbative QCD for values of q^2 far from the kinematic region where the current J can create resonances: specifically, $(m_b + m_c)\Lambda_{\text{QCD}} \ll (m_b + m_c)^2 - q^2$. For resonances containing a heavy quark, it is sufficient to take $q^2 = 0$. At one loop, $\chi_V^L = 3.7 \cdot 10^{-3}$ and $\chi_A^L = 2.2 \cdot 10^{-2}$. We also make use of the quantity $\chi_J \equiv \chi_J^T(0) - \frac{1}{2} \frac{\partial}{\partial q^2} \chi_J^L(0)$, corresponding to the combination of Π_J^T and Π_J^L that gives Π_J^{ii} at $q^2 = 0$. The full one-loop expressions for $q^2 = 0$ are

$$\begin{aligned} \chi_V(u) = \chi_A(-u) &= \frac{1}{32\pi^2 m_b^2 (1 - u^2)^5} \\ &\times [(1 - u^2)(3 + 4u - 21u^2 + 40u^3 - 21u^4 + 4u^5 + 3u^6) \\ &\quad + 12u^3(2 - 3u + 2u^2) \ln u^2], \\ \chi_V^L(u) = \chi_A^L(-u) &= \frac{1}{8\pi^2 (1 - u^2)^3} [(1 - u^2)(1 + u + u^2)(1 - 4u + u^2) - 6u^3 \ln u^2], \end{aligned} \quad (2.8)$$

where $u = m_c/m_b$ is the ratio of quark masses. For bottom and charm quark masses of $m_b = 4.5$ GeV and $m_c = 1.5$ GeV, the one-loop values of $M^2 \chi_V$ and $M^2 \chi_A$ are $1.5 \cdot 10^{-2}$ and $9.0 \cdot 10^{-3}$, respectively. One should keep in mind that $\mathcal{O}(\alpha_s)$ corrections to the bounds derived below enter as corrections to these values.

The absorptive part $\text{Im} \Pi_J^{\mu\nu}(q^2)$ is obtained by inserting on-shell states between the two currents on the right-hand side of Eq. (2.6). For any four-vector n_μ , the quantity

$n_\mu^* \Pi_J^{\mu\nu} n_\nu$ is a sum of positive-definite terms, so one can obtain strict inequalities by concentrating on the term with the two-particle intermediate state $\bar{\Lambda}_b \Lambda_c$. The contribution of $\bar{\Lambda}_b \Lambda_c$ pairs to the right-hand side of (2.7) enters as

$$\begin{aligned} n_\mu^* \text{Im} \Pi_{V-A}^{\mu\nu} n_\nu &\geq \theta(q^2 - (M+m)^2) \frac{\sqrt{k^2}}{8\pi^2 \sqrt{q^2}} \int d\Omega_p \left\{ Mm X_1 (n^* \cdot n) \right. \\ &\quad - \frac{m}{M} X_2 |p \cdot n|^2 - X_3 i \epsilon^{\mu\nu\alpha\beta} n_\mu^* n_\nu p_\alpha q_\beta - \frac{M}{m} X_4 |(q-p) \cdot n|^2 \\ &\quad \left. + X_5 (p \cdot n^*)(q-p) \cdot n + X_5^* (p \cdot n)(q-p) \cdot n^* \right\}, \end{aligned} \quad (2.9)$$

where

$$\begin{aligned} X_1 &= (\omega - 1) |F_1|^2 + (1 + \omega) |G_1|^2, \\ X_2 &= (1 + \omega) |F_2|^2 + (F_1^* F_2 + F_1 F_2^*) + (\omega - 1) |G_2|^2 + (G_1^* G_2 + G_1 G_2^*), \\ X_3 &= (F_1^* G_1 + F_1 G_1^*), \\ X_4 &= (1 + \omega) |F_3|^2 + (F_1^* F_3 + F_1 F_3^*) + (\omega - 1) |G_3|^2 - (G_1^* G_3 + G_1 G_3^*), \\ X_5 &= (1 + \omega) F_2^* F_3 + (\omega - 1) G_2^* G_3 + |F_1|^2 + F_1 F_2^* + F_1^* F_3 + |G_1|^2 - G_1 G_2^* + G_1^* G_3, \end{aligned} \quad (2.10)$$

with $\omega \equiv (M^2 + m^2 - q^2)/(2Mm)$, and the integration is over all directions of the momentum vector p . For massless leptons the differential width Eq. (2.2) is proportional to the space-space components $\text{Im} \Pi_J^{ii}$ of the two-point function, so the choice $n = (0, \hat{\mathbf{n}})$ leads to inequalities on the physically interesting form factors F_1 , G_1 , H_V , and H_A . For completeness, we also consider $n = (1, \mathbf{0})$, which leads to inequalities on the combinations

$$\begin{aligned} F_0 &= \frac{1}{M} \left[(M-m)F_1 + \frac{1}{2M}(q^2 + M^2 - m^2)F_2 - \frac{1}{2m}(q^2 - M^2 + m^2)F_3 \right] \\ G_0 &= \frac{1}{M} \left[(M+m)G_1 - \frac{1}{2M}(q^2 + M^2 - m^2)G_2 + \frac{1}{2m}(q^2 - M^2 + m^2)G_3 \right]. \end{aligned} \quad (2.11)$$

However, since n_μ can be an arbitrary q^2 -dependent four-vector, there is considerable freedom to constrain other combinations of form factors.

The analysis simplifies when Eq. (2.7) is written in terms of the conformally transformed variable z defined by

$$\frac{1+z}{1-z} = \sqrt{\frac{(M+m)^2 - q^2}{4NMm}} = \sqrt{\frac{(1+\omega)}{2N}}. \quad (2.12)$$

This expression differs from that previously used in the literature by the inclusion of the factor N ; the two agree when $N = 1$. Upon choosing the principal branch of the

square root in this expression, the change of variables $q^2 \rightarrow z$ maps the two sides of the cut $q^2 > (M+m)^2$ to the unit circle $|z| = 1$, with the rest of the q^2 plane mapped to the interior of the unit circle (Fig. 1). In particular, the real values $-\infty < q^2 \leq (M-m)^2 - 4(N-1)Mm$ and $(M-m)^2 - 4(N-1)Mm \leq q^2 < (M+m)^2$ are mapped to the real axis, $1 > z \geq 0$ and $0 \geq z > -1$ respectively. Physically, this means that the kinematic region relevant to the process $\text{vacuum} \rightarrow \overline{M}m$, $q^2 \geq (M+m)^2$, lies on the unit circle, while the region for semileptonic decay $M \rightarrow m\ell\bar{\nu}$ for massless ℓ , $0 \leq q^2 \leq (M-m)^2$, lies inside the circle on the real z -axis. Specifically,

$$\begin{aligned} z_{\min} &= -\left(\frac{\sqrt{N}-1}{\sqrt{N}+1}\right), \\ z_{\max} &= \frac{(1-\sqrt{r})^2 - 2\sqrt{r}(\sqrt{N}-1)}{(1+\sqrt{r})^2 + 2\sqrt{r}(\sqrt{N}-1)}, \end{aligned} \quad (2.13)$$

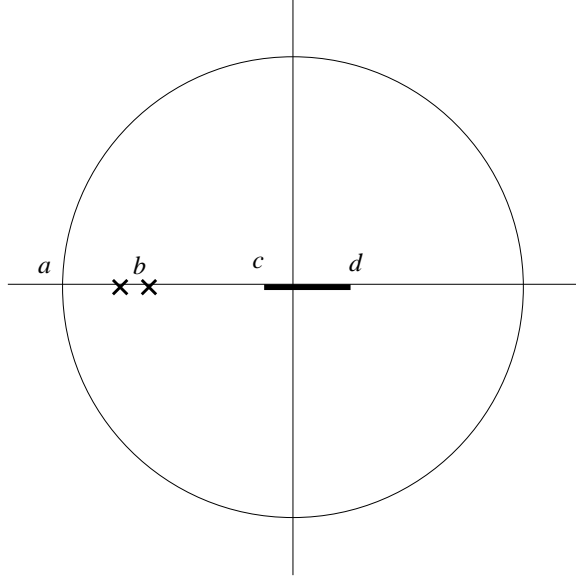


Figure 1. Important kinematic points in the z -plane for the related processes ($\text{vacuum} \rightarrow \overline{M}m$) and $M \rightarrow m\ell\bar{\nu}$ using the map Eq. (2.12). a) ($z = -1$): The branch point $q^2 = (M+m)^2$, threshold for ($\text{vacuum} \rightarrow \overline{M}m$). The two sides of the branch cut $q^2 > (M+m)^2$ map to the upper and lower halves of the unit circle, with $q^2 \rightarrow +\infty$ corresponding to $z \rightarrow +1$ along the circle. b) Location of resonant poles below the ($\text{vacuum} \rightarrow \overline{M}m$) threshold. c,d) z_{\min}, z_{\max} defined in Eq. (2.13). The segment (z_{\min}, z_{\max}) is the kinematic region for $M \rightarrow m\ell\bar{\nu}$, and N is chosen in Eq. (2.12) so that $z = 0$ lies in this interval. $q^2 \rightarrow -\infty$ corresponds to $z \rightarrow +1$ along the real axis.

where $r \equiv m/M$. Inasmuch as both $|z_{\max}|, |z_{\min}| \ll 1$, semileptonic decay possesses a small kinematic expansion parameter. One can use the free parameter N to adjust where

on the real axis the interval (z_{\min}, z_{\max}) lies, but it is clear that allowed z values are uniformly smallest when $z_{\min} \leq 0 \leq z_{\max}$, for which

$$1 \leq N \leq (M + m)^2 / (4Mm). \quad (2.14)$$

Choosing N saturates the last remaining degree of freedom allowed by the Schwarz-Christoffel transformation between the cut plane and the unit disc. N may be kinematically interpreted as the value of $(1 + \omega)/2$ for which one obtains $z = 0$ in Eq. (2.12). We explore the consequences of varying N in the next section.

Written in terms of z , the inequalities from Eqs. (2.7)-(2.10) now read

$$\frac{1}{2\pi i} \int_C \frac{dz}{z} |\phi_i(z) F_i(z)|^2 \leq 1. \quad (2.15)$$

The contour C is the unit circle. The weighting functions ϕ_i are constructed to be analytic inside the unit circle by multiplying kinematic factors by functions that are phases on the unit circle. For example,

$$\begin{aligned} \frac{q^2}{M^2} &\rightarrow [(1+r)(1-z) + 2\sqrt{Nr}(1+z)]^2 / (1-z)^2, \\ \frac{Q_-}{M^2} &\rightarrow \frac{4r}{(1-z)^2} [(\sqrt{N}-1)z + (\sqrt{N}+1)]^2, \\ \frac{Q_+}{M^2} &\rightarrow 4rN \frac{(1+z)^2}{(1-z)^2}. \end{aligned} \quad (2.16)$$

After some algebra, one obtains the weighting functions

$$\begin{aligned} \phi_i &= \sqrt{\kappa} 2^{7/2} r^{\frac{3}{2}} (1+z)^{1+p} (1-z)^{s+\frac{1}{2}} N^{\frac{3}{4}+\frac{p}{2}} \\ &\quad [(1+r)(1-z) + 2\sqrt{Nr}(1+z)]^{-(s+4)} [(\sqrt{N}-1)z + (\sqrt{N}+1)]^{\frac{3}{2}-p}, \end{aligned} \quad (2.17)$$

where κ , p , and s depend on the form factors F_i as listed in Table 1.

i	F_i	$1/\kappa$	p	s
1	F_0	$4\pi\chi_V^L$	1	0
2	F_1	$6\pi M^2\chi_V$	0	0
3	H_V	$12\pi M^2\chi_V$	0	1
4	G_0	$4\pi\chi_A^L$	0	0
5	G_1	$6\pi M^2\chi_A$	1	0
6	H_A	$12\pi M^2\chi_A$	1	1

Table 1. Factors entering Eq. (2.17) for the form factors F_i .

3. Parametrization of Form Factors

Equation (2.15) constrains the form factors F_i along the unit circle in the complex z plane, but for semileptonic decay we are interested in the physical region along the real axis, $z_{\min} \leq z \leq z_{\max}$. If the product $\phi_i(z)F_i(z)$ were analytic for $|z| < 1$, one could simply perform a Taylor expansion about $z = 0$. While the weighting functions ϕ_i are analytic inside the unit circle, the form factors F_i are not. Contributions from intermediate states with masses below the $\bar{\Lambda}_b\Lambda_c$ threshold lead to cuts and poles in $F_i(z)$ for $|z| < 1$. While we expect the contribution from cuts to be unimportant[18], the more singular nature of poles requires a careful treatment[14]. The use of Blaschke factors[21] permits one to eliminate pole contributions[15] given only their masses $\sqrt{q^2} = m_j$, which are converted to positions z_j inside the unit circle via Eq. (2.12). The Blaschke factors are defined by

$$\begin{aligned} P_V &= \prod_j \frac{(z - z_j)}{(1 - \bar{z}_j z)}, \\ P_A &= \prod_j \frac{(z - z_j)}{(1 - \bar{z}_j z)}, \end{aligned} \tag{3.1}$$

where V and A indicate the poles appropriate to the polar vector and axial vector form factors in Eq. (2.1), respectively. Resonances with spin-parity $J^P = 0^+, 1^-$ couple to form factors of the polar vector current, while resonances with $J^P = 0^-, 1^+$ couple to the axial vector current. The form factors coupled to spin-0 resonances are exactly those that are multiplied by the Lorentz structure q^μ , and consequently only appear in the differential width multiplied by the factor m_ℓ^2 . It follows that, in the massless lepton limit, only polar and axial vector resonance masses are needed in Eq. (3.1).

The usefulness of the Blaschke method lies in the fact that each factor $(z - z_j)/(1 - \bar{z}_j z)$ serves to eliminate the resonance pole behavior $1/(z - z_j)$ of the j th pole, but is unimodular for $|z| = 1$. This holds also for any product of these factors. Therefore, since each P_i is unimodular on the unit circle, one may replace $\phi_i F_i$ with $P_i \phi_i F_i$ in the bound Eq. (2.15) without changing the result. Since now both $(P_i F_i)$ and ϕ_i are analytic on the unit disc, one can perform a Taylor expansion about $z = 0$,

$$F_i(z) = \frac{1}{P_i(z)\phi_i(z)} \sum_{n=0}^{\infty} a_n z^n. \tag{3.2}$$

Substituting this expression into the modified Eq. (2.15) gives

$$\sum_{n=0}^{\infty} |a_n|^2 \leq 1. \tag{3.3}$$

It should be pointed out that one pays a price for these factors. The fact that one can eliminate pole contributions without reference to their residues means that this method must apply equally well for all allowed values of the pole residues, and therefore the bound of Eqs. (3.2) and (3.3) is necessarily weaker than the corresponding bound obtained if one knew anything about the sizes of the individual residues. In fact, the bound derived above is not very restrictive at all, until the constraints supplied by fitting to one or more experimental data points are imposed. Then the range of allowed form factors becomes surprisingly small, as was showed in Refs. [17,18].

Another strength of the parametrization Eq. (3.2) is that, when $r = m/M$ is not much less than 1, the scaled kinematic variable z defined in Eq. (2.12) is quite small. For example, if $N = 1$ the decay $\Lambda_b \rightarrow \Lambda_c \ell \bar{\nu}$ has $z_{\min} = 0$ and $z_{\max} = 0.049$. Using Eq. (3.3) it is clear that the series in Eq. (3.2) converges quickly, and one can define an uncertainty from truncating the series after only a few terms. It follows that one obtains a functional form for the form factor under consideration (Eq. (3.2)) over the whole kinematic range for semileptonic decay, with a well-controlled and small uncertainty (because z is small); only the first few parameters a_n , each of which lies in a restricted range (Eq. (3.3)), are needed.

One can do even better by allowing for the parameter $N \neq 1$. To illustrate this, let us define an approximation F_i^Q by truncating after the Q th term:

$$F_i^Q(z) = \frac{1}{P_i(z)\phi_i(z)} \sum_{n=0}^Q a_n z^n. \quad (3.4)$$

Then the maximum error incurred by truncating after Q terms is just

$$\begin{aligned} \max |F_i(z) - F_i^Q(z)| &= \max \frac{1}{|P_i(z)\phi_i(z)|} \sum_{n=Q+1}^{\infty} |a_n z^n| \\ &\leq \max \frac{1}{|P_i(z)\phi_i(z)|} \sqrt{\sum_{n=Q+1}^{\infty} |a_n|^2} \sqrt{\sum_{n=Q+1}^{\infty} z^{2n}} \\ &< \max_{z \in (z_{\min}, z_{\max})} \frac{1}{|P_i(z)\phi_i(z)|} \frac{|z^{Q+1}|}{\sqrt{1-z^2}}, \end{aligned} \quad (3.5)$$

where we have used the Schwarz inequality and Eq. (3.3). Inasmuch as $|P_i(z)\phi_i(z)|\sqrt{1-z^2}$ varies slowly over the small interval $z_{\min} \leq z \leq z_{\max}$, the truncation error is driven by $|z^{Q+1}|$. One then sees that the minimum error occurs for a value of N such that

$z_{\min} \simeq -z_{\max}$. This simple observation allows for an improvement over the corresponding expression in Refs. [17,18], which used $N = 1$ and $z_{\min} = 0$. The interval $(z_{\max} - z_{\min})$ is nearly independent of N , so z_{\max} for optimal values of N is approximately half of its value for $N = 1$. Although z is a function of N through Eq. (2.12), the Blaschke products $P_i(z)$ for fixed q^2 and pole masses are independent of N , while the weighting functions $\phi(z)$ are only weakly dependent on N . It follows that for optimal N , truncation errors are reduced by a factor of nearly 2^{Q+1} , which is appreciable even for small Q .

The reader should be reminded that the functional form Eq. (3.2) has known, bounded, and small truncation errors, regardless of the specifics of the experimental data. A form-factor expansion in $(\omega - 1)$ truncated after linear or quadratic order introduces theoretical uncertainties that can be substantial[18], and unlike (3.2) is not *a priori* guaranteed by theory to fit the data.

4. Heavy Resonances

To complete the description of the $\Lambda_b \rightarrow \Lambda_c \ell \bar{\nu}$ form factors provided by Eq. (3.2), one must construct the Blaschke products $P_i(z)$. The relevant poles are resonances below the $\bar{\Lambda}_b \Lambda_c$ threshold that couple to the $b \rightarrow c$ currents. These are the polar and axial vector B_c mesons with masses below $M_{\Lambda_b} + M_{\Lambda_c} \simeq 7.9$ GeV. Although results on B_c mesons are still very preliminary[22], their masses are reliably calculable by interpolating between the charmonium and bottomonium spectra. The quark model in a confining potential predicts a number of relevant B_c polar vector states with the spectroscopic quantum numbers 3S_1 and 3D_1 . In the bottomonium nomenclature, the analogous states are called $\Upsilon(nS)$ and $\Upsilon(nD)$, respectively. There are also relevant axial vector states, which divide into nearly degenerate pairs of 1P_1 and 3P_1 states broken only by spin-orbit and hyperfine splittings. The bottomonium analogies are respectively called $h_b(nP)$ and $\chi_{b1}(nP)$. The values obtained by various researchers[23–25] using different approximations in potential models agree within a few MeV. We use the values of Ref. [24], supplemented by values for a few higher states above the $BD^{(*)}$ threshold but below the $\bar{\Lambda}_b \Lambda_c$ threshold[26]. Although the masses of the latter states do not yet appear in the published literature, their calculation is no more difficult than that of those already published; however, one should keep in mind that the simple nonrelativistic bound-state picture for such B_c resonances is no longer fully justified: The coupling of open channels to the resonances above the BD threshold can modify the details of the mass spectrum. Nevertheless, experience from the J/ψ and Υ

systems shows that such calculations give a reasonable account of masses above the $\bar{D}D$ and $\bar{B}B$ thresholds. We present the B_c pole mass values used in Table 2.

Type	Source	Masses (GeV)
Vector	Ref. [24]	6.337, 6.899, 7.012, 7.280
	Ref. [26]	7.350, 7.594, 7.646, 7.872 7.913
Axial	Ref. [24]	6.730, 6.736, 7.135, 7.142
	Ref. [26]	7.470, 7.470, 7.757, 7.757

Table 2. Assumed B_c pole masses used in this work. A complete set of masses for either parity consists of the values from Ref. [24], together with the newly-computed values from Quigg[26].

The truncation errors on our parametrizations depend on the Blaschke factors only through the endpoint values $P(z_{\min})$ and $P(z_{\max})$, because empirically the maximum truncation errors from Eq. (3.5) occur at either $z = z_{\min}$ or z_{\max} . These values of P do not depend on N , but they do depend on the masses of states between the BD and $\bar{\Lambda}_b\Lambda_c$ thresholds. We present the truncation errors for $Q = 2$ (a two-parameter description if given the overall normalization, or three parameters otherwise) in Table 3. Truncation errors for $Q = 3$ are roughly a factor of 40 times smaller because of the additional suppression of about $z_{\max}^{N=1}/2$ described in Sec. 3. To compare these absolute truncation errors to the expected size of the form factors, note that heavy quark symmetry predicts the normalization of F_1 and G_1 at zero recoil to be unity, while the other form factors are $\mathcal{O}(1/m_c)$ in this limit[4]. Empirically, the value $N = 1.09$ minimizes the truncation errors, although this number may change slightly depending on the actual values of $P(z_{\min})$ and $P(z_{\max})$. These truncation errors are substantially smaller than those for $N = 1$, which is 28% for F_1 , for example. Randomly altering the resonance masses by 20–50 MeV alters the truncation errors presented in Table 3 by less than one part in ten in each case, indicating the insensitivity of the errors to the particular assumptions of the potential model used to compute B_c masses.

F_i	(Max. Trunc. error) $\cdot 10^2$	N_{ideal}
F_0	4.0	1.088
F_1	5.1	1.088
H_V	20.0	1.089
G_0	4.3	1.089
G_1	6.6	1.088
H_A	25.7	1.089

Table 3. *Truncation errors from Eqs. (3.4) and (3.5) of the $\Lambda_b \rightarrow \Lambda_c \ell \bar{\nu}$ form factors for the pole masses given in Table 2 with $Q = 2$. N_{ideal} is the value of N for which these errors are minimized. Including all other known corrections multiplies the truncation errors by the coefficient $B \leq 1.4$ described in the text.*

Finally, we briefly commented in Sec. 3 that the effect of branch cuts due to non-resonant on-shell intermediate states connecting the vacuum to $\bar{\Lambda}_b \Lambda_c$ are not numerically significant, just as in $\bar{B} \rightarrow D^{(*)} \ell \bar{\nu}$. In Ref. [18] their effects were accommodated by relaxing the bound (3.3) to $\Sigma |a_n|^2 \leq B^2$, with $B \leq 1.05$. In the present case, however, the $\bar{\Lambda}_b \Lambda_c$ threshold is higher than the $BD^{(*)}$ threshold, and so many more cuts are possible. To argue that their total effect is still negligible requires a more detailed analysis than appears in [18].

We begin with the observation that multiparticle intermediate states connect the current J^μ to $\bar{\Lambda}_b \Lambda_c$, and thus appear as loop diagrams. Each additional intermediate state introduces a loop and large- N_{color} factor of $1/(16\pi^2 N_c^{1/2})$, so we limit ourselves to two-particle intermediates. In reference [18], we modeled the contribution of such a state with a square-root cut, as follows. If the combined mass of the intermediate particles corresponds to $z = z_{\text{cut}}$, the cut contribution to B is

$$\delta B = \left[\frac{1}{2\pi} \int_0^{2\pi} d\theta |g_{\text{cut}}(z)\phi(z)|^2 \right]^{1/2}, \quad (4.1)$$

where $z = e^{i\theta}$, $\phi(z)$ is the weighting function, and

$$g_{\text{cut}}(z) = \frac{4c\sqrt{r}}{M_{\Lambda_b}} \left(\frac{\sqrt{(z - z_{\text{cut}})(1 - z z_{\text{cut}})}}{(1 - z)(1 - z_{\text{cut}})} - \frac{1 + z}{2(1 - z)} \right) \quad (4.2)$$

models the cut.

The coupling constant c may be written as $c = \hat{f}\hat{g}/8\pi$, where \hat{f} is the coupling between the current and the two-particle intermediate state, \hat{g} is the overlap between these states and $\bar{\Lambda}_b \Lambda_c$, and the 8π comes from the loop.

Two-particle intermediate states with strangeness are OZI suppressed, so the only kinematically allowed possibilities are $B - D$ resonances and states with one B_c resonance and one light unflavored meson. We may further limit our consideration to S -waves only, since higher partial amplitudes are suppressed by powers of the available three-momentum, $\mathcal{O}(\Lambda_{\text{QCD}})$ because we are in the resonance region, divided by the center-of-mass energy, $\mathcal{O}(M_B + M_D)$. Furthermore, two-particle intermediates in which one of the particles has

strong isospin (such as $B_c\pi$) are heavily suppressed by isospin-breaking coefficients, and will be ignored.

With these restrictions, the decay $\bar{B} \rightarrow D^*\ell\bar{\nu}$ admits only two very short cuts in the 1^- channel ($B_c(^3P_1)\eta$ and $B_c(^1P_1)\eta$), with $z_{\text{cut}} \approx -0.88$, and three in the 1^+ channel, with the lowest being $B_c^*\eta$ with $z_{\text{cut}} = -0.48$. There are anomalous cuts starting at $z \approx -0.35$, but they are proportional to a $B^*-B-\pi$ coupling g^2 that is probably quite small[16]. $\bar{B} \rightarrow D\ell\bar{\nu}$ has no cuts in the relevant 1^- channel, anomalous or otherwise. These branch cuts lead to even smaller uncertainties for $\bar{B} \rightarrow D^{(*)}\ell\bar{\nu}$ than anticipated in Ref. [18]. On the other hand, once the threshold is raised to the $\Lambda_b + \Lambda_c$ mass, many more cuts occur. We count 32 in the 1^- channel and 28 in the 1^+ channel, including such exotic combinations as $B_c(2^3P_0(6700)) + h_1(1170)$. To justify our neglect of so many cuts requires a more careful study.

The great majority of cuts in either channel arise from a B_c resonance and a light unflavored meson. To get a rough estimate of their combined contribution, we take them all to have the same coupling c , compute the contribution to B of each state separately, and add them in quadrature (to simulate random phases between the various cuts). We find that B is only increased to $1 + 0.5c$ for the 1^- channel and $1 + 0.6c$ for the 1^+ channel. Furthermore, we expect $c = \hat{f}\hat{g}/8\pi$ to be very small. To judge the typical size of \hat{f} , for example, we can extract the coupling $\hat{f}_{\psi\eta}$ of a vector current to the J/ψ - η state from charmonium radiative decay data. Using a phenomenological Lagrangian term

$$\delta\mathcal{L} = ie\hat{f}_{\psi\eta}M_{\psi}\psi^\mu A_\mu\eta \quad (4.3)$$

gives a coupling $\hat{f}_{\psi\eta} < 10^{-2}$, while bottomonium data gives an even smaller bound on $\hat{f}_{\Upsilon\eta}$. Taking the interpolated value of $\hat{f}_{B_c\eta}$ as representative, we conclude that cuts involving B_c resonances give negligible contribution to B .

On the other hand, the intermediate states consisting of a B - D pair may have much larger couplings, with $\hat{f}\hat{g}$ conceivably of order one, but the cuts begin much closer to the $\bar{\Lambda}_b\Lambda_c$ threshold and are fewer in number (six for the 1^- channel, with minimum $z_{\text{cut}} = -0.55$, three for the 1^+ channel, with minimum $z_{\text{cut}} = -0.39$). Added in quadrature, the bounding parameter B in the vector (axial) channel receives a $0.12c$ ($0.18c$) correction. However, since our uncertainty estimates to obtain B [18] are added in quadrature, the conservative total correction to Eq. (3.3) given by $B \leq 1.4$ remains unchanged in this work, even if $c = \mathcal{O}(1)$. In addition to multi-particle cuts, these uncertainty estimates

include corrections to the heavy quark limit, choices of quark mass values, and $\mathcal{O}(\alpha_s)$ perturbative corrections, as well as others. A value of $B = 1.4$ has the effect of increasing all of our truncation errors by a factor of 1.4; such increases on a few-percent truncation error do not hamper our conclusions.

5. Implications for Meson Decays

The freedom to choose N in Eq. (2.12) has significant implications for semileptonic meson decays like $\bar{B} \rightarrow D^{(*)} \ell \bar{\nu}$ and $\bar{B} \rightarrow \pi \ell \bar{\nu}$. For $\bar{B} \rightarrow D \ell \bar{\nu}$ and $\bar{B} \rightarrow D^* \ell \bar{\nu}$, the form factors defined by

$$\begin{aligned}\langle D^*(p', \epsilon) | V^\mu | \bar{B}(p) \rangle &= i g \epsilon^{\mu\alpha\beta\gamma} \epsilon_\alpha^* p'_\beta p_\gamma \\ \langle D^*(p', \epsilon) | A^\mu | \bar{B}(p) \rangle &= f_0 \epsilon^{*\mu} + (\epsilon^* \cdot p) [a_+(p + p')^\mu + a_-(p - p')^\mu] \\ \langle D(p') | V^\mu | \bar{B}(p) \rangle &= f_+(p + p')^\mu + f_-(p - p')^\mu\end{aligned}\tag{5.1}$$

and

$$F_1 = \frac{1}{m} \left[2q^2 k^2 a_+ - \frac{1}{2}(q^2 - M^2 + m^2) f_0 \right],\tag{5.2}$$

where now $M = M_B$ and $m = M_{D^{(*)}}$, have weighting functions

$$\begin{aligned}\phi_i &= M^{2-s} \sqrt{\kappa n_f} 2^{2+p/2} [r(1+z)]^{\frac{1+p}{2}} (1-z)^{s-\frac{3}{2}} N^{\frac{1}{2}+\frac{p}{4}} \\ &[(1+r)(1-z) + 2\sqrt{Nr}(1+z)]^{-(s+p)} [(\sqrt{N}-1)z + (\sqrt{N}+1)]^{\frac{p}{2}},\end{aligned}\tag{5.3}$$

where n_f is an isospin Clebsch-Gordan factor that is 2 for $\bar{B} \rightarrow D^{(*)} \ell \bar{\nu}$ and $\frac{3}{2}$ for $\bar{B} \rightarrow \pi \ell \bar{\nu}$, $r \equiv m/M$, and the values of κ , p , and s are given in Table 4. The parameters p and s here do not have precisely the same origin as those in Eq. (2.17). Equation (5.3) agrees with Ref. [18] in the limit $N \rightarrow 1$.

i	F_i	$1/\kappa$	p	s
0	f_0	$12\pi M^2 \chi_A$	1	3
1	F_1	$24\pi M^2 \chi_A$	1	4
2	g	$12\pi M^2 \chi_V$	3	1
3	f_+	$6\pi M^2 \chi_V$	3	2

Table 4. *Factors entering Eq. (5.3) for the meson form factors F_i .*

From the discussion in Sec. 3, one expects that by choosing the optimal value between $N = 1.10$ and 1.12 (the exact value depends upon the form factor), the truncation errors

for a three-parameter description should be reduced by roughly a factor of 8 over the $N = 1$ values in Ref. [18], while the truncation errors for a two-parameter fit should be reduced by a factor of about 4. From direct calculation, these numbers are 6.1–7.2 and 3.3–3.7, in accord with expectations. Since one of the parameters is determined from the normalization of the form factor at zero recoil by heavy quark symmetry, the $N \simeq 1.1$ choice provides a *one*-parameter description of each of the form factors with truncation errors (relative to the normalization at zero recoil) of 6.4%, 5.0%, 2.9%, and 30.9% for f_+ , f_0 , g , and F_1 , respectively. For the form factor g , for example, the conclusion is that using the normalization at zero recoil (which determines a_0) plus the slope at the same point (which determines a_1), one obtains the shape of g over the entire kinematic range with a theoretical error of no more than 2.9%. Uncertainties like corrections to heavy quark symmetry, perturbative QCD corrections, and so on are expected to increase this theoretical error to no more than 4.1% and possibly much less[18]. For example, the truncation error vanishes at zero recoil, where the normalization is known.

We exhibit the possible shapes of $g(\omega)/g(1)$ in Fig. 2. The lowest curve corresponds to the saturation of Eq. (3.3) by $a_1 = -1$, while the top curve corresponds to $a_1 = 0.115$, the largest value allowed by the the Bjorken inequality[27] on the slope of the Isgur-Wise function improved by $\mathcal{O}(\alpha_s)$ corrections[28]. Intermediate curves correspond to equally spaced values of a_1 .

The form factor f_+^π defined by replacing the D meson in Eq. (5.1) with a pion has the same weighting function ϕ_+ as f_+^D , but with the D mass replaced with the pion mass and $\chi_V = 9.5 \cdot 10^{-3}/m_b^2$. The Blaschke factor for the pion form factor is $P^\pi = (z - z_*)/(1 - z z_*)$, with z_* corresponding to the B^* mass, the sole resonance below threshold. One might expect a suitable choice of N to lead to $|z_{min}|, |z_{max}|$ of about half the $N = 1$ value of $z_{max}^{N=1} \simeq 0.5$. Unfortunately, one cannot ignore the variation of $P(z)\phi(z)\sqrt{1 - z^2}$ over the kinematic range, so the reduction in truncation errors is less spectacular than in the $B \rightarrow D$ system. It is nevertheless a significant improvement: Where for $N = 1$, a four-parameter description implied an absolute truncation error of 1.35, for $N = 2.1$ the absolute truncation error is 0.37. A five-parameter description yields, for $N = 2.27$, a 0.11 truncation error. Even for a three-parameter description, the absolute truncation error at $N = 1.86$ is 1.19 over the large kinematic range of $\bar{B} \rightarrow \pi \ell \bar{\nu}$. In typical models, $f_+^\pi(q^2)$ varies from around 0.3 at $q^2 = 0$ [29] to order 10 at $q^2 = (M_B - m_\pi)^2$ [16]. Other models may give smaller values of $f_+^\pi(q_{max}^2)$ or fall off rapidly away from q_{max}^2 , and then it is useful and straightforward to choose N in order to minimize the truncation errors *relative* to particular points fixed by a model, instead of the absolute errors quoted above.

6. Conclusions

The analysis of dispersion relations and analyticity properties of strong-interaction amplitudes, once ubiquitous in particle theory, can still yield a surprising amount of information about heavy hadron transitions. For the semileptonic decays considered in this paper, this stems from a two-part procedure: First, the perturbative calculation of a two-point function, performed in an unphysical kinematic regime where the calculation is reliable, is connected by crossing symmetry and a dispersion relation to the QCD form factors of interest. Second, some complex analysis consisting of a conformal transformation, a multiplication by Blaschke functions, and a Taylor expansion, produces a simple parametrization for the form factors in the physical region.

In the current work we have presented an improvement of the conformal transformation that decreases the number of parameters necessary for an accurate description of the form factors over a given kinematic range. We have computed the explicit parametrizations for the form factors of the decay $\Lambda_b \rightarrow \Lambda_c \ell \bar{\nu}$, and have recomputed, using the new conformal transformation, the parametrizations of the mesonic decay form factors for $\bar{B} \rightarrow D^{(*)} \ell \bar{\nu}$ and $\bar{B} \rightarrow \pi \ell \bar{\nu}$.

In particular, for a two-parameter description of $\Lambda_b \rightarrow \Lambda_c \ell \bar{\nu}$ form factors (utilizing heavy quark symmetry for the normalization), we find truncation errors of 4–7% for the form factors associated with transversely polarized lepton pairs, and errors of 20–26% for the longitudinally polarized combinations. These numbers would have been much larger without the technical improvement to the conformal map Eq. (2.12), owing to the large number of B_c resonance masses below the $\bar{\Lambda}_b \Lambda_c$ threshold. The truncation errors are seen to be quite insensitive to the exact locations of the B_c poles, so our results do not depend on the detailed assumptions of a particular potential model calculation.

Constraints for the decays $\bar{B} \rightarrow D^{(*)} \ell \bar{\nu}$, which were already quite restrictive from earlier work, become more so using this technical improvement. In particular, we showed that one can obtain a one-parameter fit to all of these form factors except F_1 good to 3–6%, using the normalization from heavy quark symmetry. A description of the form factor f_+ of $\bar{B} \rightarrow \pi \ell \bar{\nu}$ good over the entire kinematic range to an absolute uncertainty of 0.37 requires only four parameters. Relative to the expected size of f_+ , this represents a small fractional uncertainty in the pole-dominated region. In addition, if the normalization of f_+ at more than one kinematic point is known, the envelope of allowed parametrizations becomes quite restricted, even for small q^2 [16].

These conclusions follow only from very general properties of QCD and S -matrix amplitudes. They do not rely on such potentially useful information as the contribution of excited states above threshold to the dispersion relation, or the actual contribution (residues) of heavy resonances below threshold to singularities of the form factors. One might therefore expect only very weak constraints to arise; instead one is rewarded with strong restrictions on the shape of the form factors. In this paper, our treatment has been somewhat mathematical. A physical understanding of why the restrictions are so strong, and what role the small but apparently natural variable z plays, would be of considerable interest. Further detailed computations compatible with the QCD dispersion constraints may yield restrictions that are better still.

Acknowledgments

We would like to thank Ben Grinstein and Aneesh Manohar for valuable conversations, Vivek Sharma for a discussion of current experimental information, and especially Chris Quigg, who computed a number of B_c mass eigenvalues used in this paper. This work is supported in part by the Department of Energy under contract DOE-FG03-90ER40546.

References

- [1] N. Isgur and M.B. Wise, Phys. Lett. B **232** (1989) 113 and Phys. Lett. B **237** (1990) 527.
- [2] E. Eichten and B. Hill, Phys. Lett. B **234** (1990) 511.
- [3] M. B. Voloshin and M. A. Shifman, Yad. Fiz. **47**, (1988) 801 [Sov. J. Nucl. Phys. **47** (1988) 511].
- [4] N. Isgur and M. B. Wise, Nucl. Phys. **B348** (1991) 276.
- [5] M. E. Luke, Phys. Lett. B **252** (1990) 447.
- [6] H. Georgi, B. Grinstein, and M. B. Wise, Phys. Lett. B **252** (1990) 456.
- [7] D. Buskulic *et al.* (ALEPH Collaboration), Phys. Lett. B **359** (1995) 236.
- [8] V. Sharma, private communication.
- [9] ALEPH Collaboration, contribution to the International Europhysics Conference on High Energy Physics, Brussels, Belgium, July 1995, EPS0753;
DELPHI Collaboration, CERN-PPE/95-54;
OPAL Collaboration, CERN-PPE/95-051.
- [10] CDF Collaboration, HyperText document <http://www-cdf.fnal.gov/physics/new/bottom/cdf3395/cdf3395.html>.
- [11] N.N. Meiman, Sov. Phys. JETP **17** (1963) 830;
S. Okubo, Phys. Rev. **D3** (1971) 2807;
S. Okubo and I. Fushih, Phys. Rev. **D4** (1971) 2020;
V. Singh and A.K. Raina, Fortschritte der Physik **27** (1979) 561.
- [12] C. Bourrely, B. Machet, and E. de Rafael, Nucl. Phys. **B189** (1981) 157.
- [13] E. de Rafael and J. Taron, Phys. Lett. B **282** (1992) 215.
- [14] E. Carlson, J. Milana, N. Isgur, T. Mannel, and W. Roberts, Phys. Lett. B **299** (1993) 133;
A. Falk, M. Luke, and M. B. Wise, Phys. Lett. B **299** (1993) 123;
B. Grinstein and P. Mende, Phys. Lett. B **299** (1993) 127;
C. Dominguez, J. Körner, and D. Pirjol, Phys. Lett. B **301** (1993) 373.
- [15] E. de Rafael and J. Taron, Phys. Rev. **D50** (1994) 373;
I. Caprini, Z. Phys. C **61** (1994) 651, Phys. Lett. B **339** (1994) 187.
- [16] C.G. Boyd, B. Grinstein, and R.F. Lebed, Phys. Rev. Lett. **74** (1995) 4603.
- [17] C.G. Boyd, B. Grinstein, and R.F. Lebed, Phys. Lett. B **353** (1995) 306.
- [18] C.G. Boyd, B. Grinstein, and R.F. Lebed, Nucl. Phys. **B461** (1996) 493.
- [19] L. Lellouch, Marseille preprint CPT-95/P.3236 [hep-ph/9509358] (unpublished).
- [20] J. G. Körner and M. Krämer, Phys. Lett. B **275** (1992) 495.
- [21] P. Duren, *Theory of H^p Spaces*, Academic Press, New York, 1970.
- [22] ALEPH Collaboration, Report No. EPS0407, contribution to the International Europhysics Conference on High Energy Physics, Brussels, Belgium, July, 1995.

- [23] V.V. Kisilev, A.K. Likhoded, and A.V. Tkabladze, Phys. Rev. **D51** (1995) 3613.
- [24] E.J. Eichten and C. Quigg, Phys. Rev. **D49** (1994) 5845.
- [25] Y.-Q. Chen and Y.-P. Kuang, Phys. Rev. **D46** (1992) 1165.
- [26] Chris Quigg, private communication.
- [27] J.D. Bjorken, in *Proceedings of the 4th Recontres de Physique de la Vallée d'Aoste*, La Thuille, Italy, 1990, ed. M. Greco (Editions Frontières, Gif-Sur-Yvette, France, 1990);
N. Isgur and M.B. Wise, Phys. Rev. **D43** (1991) 819;
J.D. Bjorken, I. Dunietz, and J. Taron, Nucl. Phys. **B371** (1992) 111.
- [28] C.G. Boyd, B. Grinstein, and A.V. Manohar, U.C. San Diego preprint No. UCSD/PTH 95-19 [hep-ph/9511233] (to appear in Phys. Rev. D).
- [29] M. Wirbel, B. Stech, and M. Bauer, Zeit. Phys. **C29** (1985) 637;
N. Isgur and D. Scora, Phys. Rev. **D52** (1995) 2783.

Figure Captions

Figure 1. Important kinematic points in the z -plane for the related processes (vacuum $\rightarrow \overline{M}m$) and $M \rightarrow m\ell\bar{\nu}$ using the map Eq. (2.12). a) ($z = -1$): The branch point $q^2 = (M+m)^2$, threshold for (vacuum $\rightarrow \overline{M}m$). The two sides of the branch cut $q^2 > (M+m)^2$ map to the upper and lower halves of the unit circle, with $q^2 \rightarrow +\infty$ corresponding to $z \rightarrow +1$ along the circle. b) Location of resonant poles below the (vacuum $\rightarrow \overline{M}m$) threshold. c,d) z_{\min}, z_{\max} defined in Eq. (2.13). The segment (z_{\min}, z_{\max}) is the kinematic region for $M \rightarrow m\ell\bar{\nu}$, and N is chosen in Eq. (2.12) so that $z = 0$ lies in this interval. $q^2 \rightarrow -\infty$ corresponds to $z \rightarrow +1$ along the real axis.

Figure 2. The one-parameter description of the $\bar{B} \rightarrow D^*\ell\bar{\nu}$ form factor $g(\omega)/g(1)$, plotted as a function of velocity transfer ω , for a set of values of the parameter a_1 . The lowest curve corresponds to the saturation of Eq. (3.3) by $a_1 = -1$, while the top curve corresponds to $a_1 = 0.115$, the largest value allowed by the α_s -improved Bjorken inequality[27,28]. Intermediate curves correspond to equally spaced values of a_1 .

Fig. 2: Form Factor $g(w)/g(1)$

